The Mobile Flavin of 4-OH Benzoate Hydroxylase

Domenico L. Gatti, Bruce A. Palfey, Myoung Soo Lah,*
Barrie Entsch, Vincent Massey, David P. Ballou,
Martha L. Ludwig†

Para-hydroxybenzoate hydroxylase inserts oxygen into substrates by means of the labile intermediate, flavin C(4a)-hydroperoxide. This reaction requires transient isolation of the flavin and substrate from the bulk solvent. Previous crystal structures have revealed the position of the substrate *para*-hydroxybenzoate during oxygenation but not how it enters the active site. In this study, enzyme structures with the flavin ring displaced relative to the protein were determined, and it was established that these or similar flavin conformations also occur in solution. Movement of the flavin appears to be essential for the translocation of substrates and products into the solvent-shielded active site during catalysis.

Many enzyme-catalyzed reactions require insulation of the reacting species from aqueous solvent. This is often achieved by induced fit rearrangements of protein loops or domains (*1*). We have studied the accessibility of substrates to the active site of *para*-hydroxybenzoate hydroxylase (PHBH), a bacterial flavoprotein. PHBH (E.C. 1.14.13.2) catalyzes the monooxygenation of *p*-hydroxybenzoate (*p*-OHB), formed during the biodegradation of lignin, to 3,4-dihydroxybenzoate (Fig. 1). The latter compound is a metabolite in several aromatic degradation pathways (*2*). PHBH is the prototype for a number of flavoprotein monooxygenases that catalyze similar hydroxylation reactions, in which molecular oxygen is cleaved without the intervention of a metal ion (*3*). The environment provided by the enzyme must be critical, because free flavins are not capable of carrying out such reactions. The key intermediate in the catalytic cycle of PHBH is the flavin C(4a)-hydroperoxide, which is unstable in protic solvents (*4*). This intermediate is generated by the reaction of O_2 with the reduced flavin of the *p*-OHB · enzyme complex (reaction 2 of Fig. 1) (*5*) in the environment of the active site, where the solvent-shielded hydroperoxide is positioned for reaction with the substrate (*6*). Coupling of substrate hydroxylation to flavin reoxidation is further promoted by a decrease in the rate of substrate release from the reduced enzyme (5000 times slower than when the enzyme is oxidized) (*7*). Previous crystallographic studies have shown substrate (Fig. 2) or product enclosed in the active site (*8*) but have not shown how the substrate enters or leaves its binding site.

The flavin ring can adopt two positions in the active site of PHBH. An alternate conformation was first detected in the structure of the *p*-OHB complex with the mutant enzyme $Tyr^{222} \rightarrow Phe^{222}$ (Y222F) (Table 1) (*9*), where the electron density reveals that the isoalloxazine ring has moved outward, away from the substrate, into a more solvent-accessible region (Fig. 3). Water molecules fill the volume originally occupied by the pyrimidine portion of the flavin; the substrate and the side chain of residue 222 are not displaced when the flavin moves (Fig. 3B). Examination of the electron density at the active site reveals that the observed structure actually represents a mixture of the "in" and "out" orientations, as shown in Fig. 3A. Crystallographic refinement with two alternate conformations of the flavin ring (*10–13*) results in a ratio of about 7:3 for the occupancies of the out and in positions, respectively. In the mutant Y222F, an interaction between the isoalloxazine O(4) and Arg^{220} helps to stabilize the flavin in the out position.

The out conformation of the flavin was also observed in the wild-type enzyme in complex with an alternative substrate, 2,4-dihydroxybenzoate (2,4-DOHB) (Fig. 4).

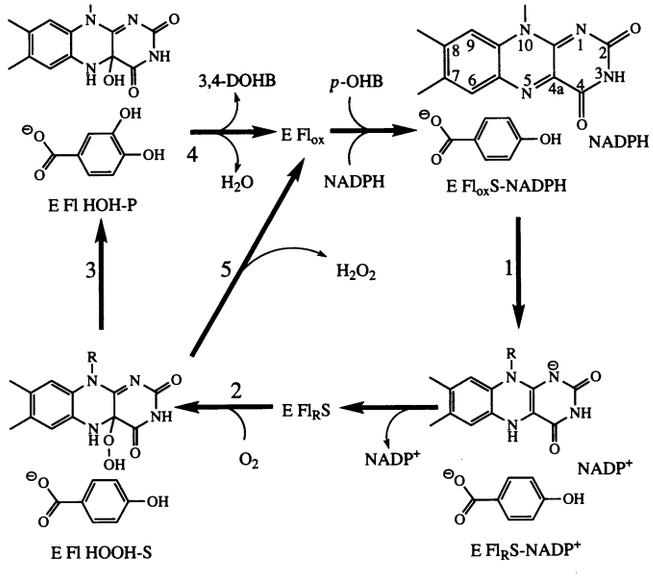

Fig. 1 (right). The catalytic cycle of PHBH. The numbers near the arrows refer to reaction steps determined by stopped-flow kinetic analysis: (1) reduction of the flavin in the presence of substrate; (2) formation of the 4(a)-flavin hydroperoxide species; (3) substrate hydroxylation; (4) dehydration of the flavin 4(a)-hydroxide; (5) uncoupling with release of hydrogen peroxide. The abbreviations used are: E Fl HOOH, C(4a)-hydroperoxide of the enzyme-bound FAD; E Fl HOH, C(4a)-hydroxide of the enzyme-bound FAD; Fl_{ox}, oxidized flavin; Fl_R, reduced flavin. The numbering of the isoalloxazine ring atoms is shown in the drawing of the oxidized flavin (upper right).

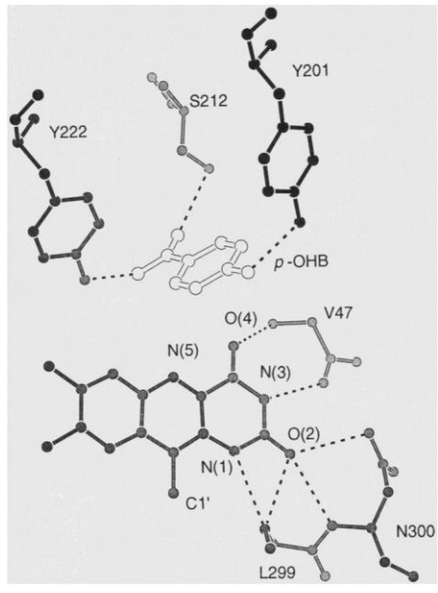

Fig. 2 (far right). Features of the active site of wild-type PHBH with the substrate, *p*-OHB, bound (*8*, *22*). Several hydrogen bonds connect the protein to the pyrimidine portion of the flavin ring: The backbone of Val^{47} interacts with O(4) and N(3), and residues Leu^{299} and Asn^{300} interact with O(2) and N(1). The dimethylbenzene end of the flavin is exposed to the solvent. The *si* side of the flavin ring, facing away from the viewer, is in direct contact with backbone atoms of a short loop(residues 43 to 48), whereas several water molecules (not shown) contact the *re* side (facing the viewer). *Para*-hydroxybenzoate occupies a pocket located near the C(4a) and O(4) atoms of the flavin. Its carboxylate group is held in place by interactions with the guanidinium of Arg^{214} (as shown in Fig. 4) and by hydrogen bonding to the OH groups of Ser^{212} and Tyr^{222}. The 4-hydroxyl of the substrate is hydrogen-bonded to the carbonyl of Pro^{293} (not shown) and to the hydroxyl group of Tyr^{201}.

The electron density in the region of the dimethylbenzene ring is very well defined in this crystal structure (Table 1); no evidence of other conformations was observed. Some of the key interactions that maintain the flavin in the out position in the wild-type enzyme · 2,4-DOHB complex differ from those stabilizing the out position of the flavin in the Y222F mutant. In particular, in the 2,4-DOHB complex, the out orientation of the flavin is favored by a strong hydrogen bond between N(3) of the flavin and the 2-OH of 2,4-DOHB (Fig. 4).

Spectroscopic measurements provide evidence for more than one conformational state of the PHBH flavin in solution. Perturbations of the optical spectrum of flavin-adenine dinucleotide (FAD) are induced by the addition of substrates and other ligands to the oxidized enzyme. The difference spectrum produced by binding *p*-OHB to Y222F has characteristic peaks at 390 and 480 nm (Fig. 5); addition of 2,4-DOHB to the wild-type enzyme produces a more intense difference spectrum with the same features. In contrast, in the wild-type PHBH · *p*-OHB complex, where the flavin adopts the in conformation, a smaller and qualitatively different spectral change is observed on addition of *p*-OHB. The occurrence and magnitude of the difference peaks at 390 and 480 nm correlate with the population of the flavin in the out position as detected in the crystal structures of the complexes Y222F · *p*-OHB and wild-type PHBH · 2,4-DOHB, and can be interpreted as a signature for interactions between the substrate and a displaced flavin.

The orientation of the flavin in PHBH in solution was also examined by chemical modification with a flavin analog carrying a photoreactive azido group. For these studies, 6-azido-FAD was incorporated into PHBH (*14*). When irradiated with visible light, the azido group is converted to a highly reactive nitrene (*15*). We determined the extent of photolabeling of the wild-type enzyme by the nitrene in the presence or absence of substrates (*14*).

D. L. Gatti, B. A. Palfey, M. S. Lah, V. Massey, D. P. Ballou, M. L. Ludwig, Department of Biological Chemistry and Biophysics Research Division, University of Michigan, Ann Arbor, MI 48109, USA.
B. Entsch, Department of Biochemistry and Microbiology, University of New England, Armidale, NSW 2351, Australia.

*Present address: Department of Chemistry, Hanyang University, 396 Taehakdong Ansan, Kyunggido, Korea.
†To whom correspondence should be addressed.

Table 1. Summary of data sets and crystallographic refinements (WT, wild-type PHBH). Data sets were collected at 22°C with a dual area detector (Area Detector Systems). The space group was $C222_1$ for all crystals of the *Pseudomonas aeruginosa* enzyme. Cell dimensions, which were insensitive to the addition of substrates or inhibitors, were: a = 71.81 ± 0.10 Å, b = 146.38 ± 0.29 Å, c = 88.20 ± 0.17 Å (mean ± SD). Crystals of the *P. aeruginosa* enzyme are highly isomorphous to those of the *P. fluorescens* enzyme (*8*), which therefore was used as the starting model. The first steps of refinement used only the reflections between 5 and 2 Å. After initial adjustment of the coordinates, in which the model (not containing water molecules) was treated as a rigid body, the positional parameters were refined by simulated annealing (by use of the slow-cool protocol) from 1000 K with X-PLOR (*10*). These steps were followed by independent refinement of the thermal and occupancy parameters. Water molecules were added interactively (*13*). A final refinement of all independent parameters was done after inclusion of the reflections in the range 15 to 5 Å, in association with the computation of a mask to account for the contribution of the bulk solvent to the x-ray term.

Parameter	Y222F · *p*-OHB	WT · 2,4-DOHB	WT · *p*-OHB–Br^-	WT · 2,4-DOHB–Br^-
Resolution (Å)	15 to 2.0	15 to 2.1	15 to 2.0	15 to 2.3
Unique reflections	27,601	25,883	31,516	20,897
Completeness (%)	86.95	96.64	99.47	99.54
⟨Redundancy⟩	3.5	7.22	7.10	8.73
$\langle I/\sigma I\rangle$	6.8	8.73	10.01	7.32
R_{sym}*	11.92	8.65	9.68	11.35
Final R†	0.205	0.168	0.173	0.164
Solvents	159	169	208	168

*R_{sym}: $\Sigma|\langle I\rangle - I|/\Sigma|\langle I\rangle|$ ($\langle I\rangle$ = mean intensity of symmetry equivalent reflections). †R: $\Sigma(h)||F_{obs}(h)| - k|F_c(h)||/\Sigma(h)|F_{obs}(h)|$ (k = scale factor).

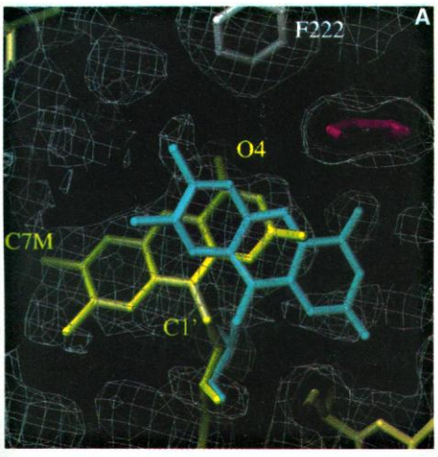

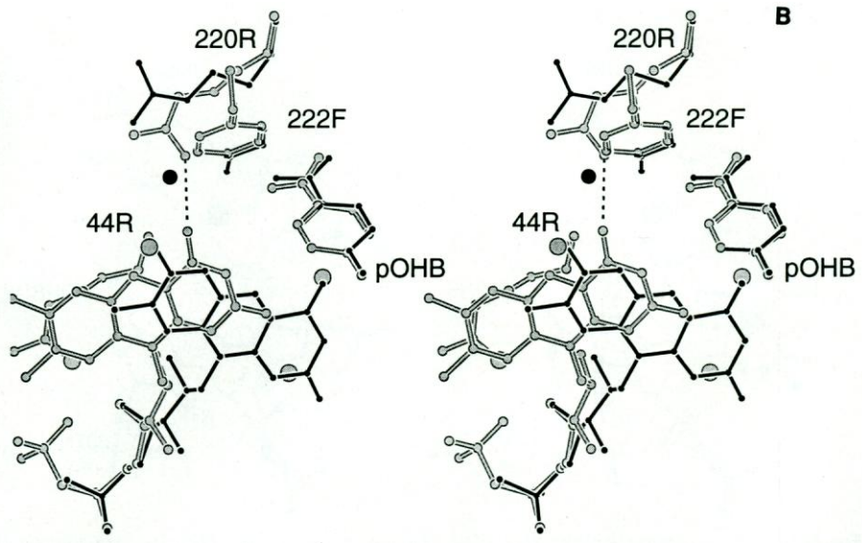

Fig. 3 (**A**) Electron densities showing the two modes of flavin binding in the mutant Y222F. The flavin ring in the outer position is modeled in yellow; that in the inner position is blue. Substrate (red) is viewed edge on, above the inner flavin. The electron densities were computed with coefficients $w|F_{obs}|\ \exp(i\phi_{comb})$ (*23*) and are contoured at 0.3 σ. The highest density is concentrated in the region of overlap between the two positions of the flavin. Occupancy of the in conformation is evident from the distribution of density for the ribityl side-chain position C1′ and from the density corresponding to the 7-CH_3 group of the in conformer. (**B**) Comparisons of the structures of wild-type PHBH (solid bonds) and the mutant Y222F (shaded bonds) (*22*). This stereoview shows the displacement of the flavin that is observed in the mutant. Hydrogen bonds between the protein and the pyrimidine portion of the flavin ring, shown in Fig. 2, are partly replaced in the out conformation by interactions with solvent (shaded circles); one of these water molecules bridges the flavin O(2) to the backbone NH 299 of the first turn of helix H10. In the wild-type enzyme, the hydroxyl of Tyr^{222} is hydrogen-bonded to a water molecule (filled) that bridges Arg^{220} to the backbone NH-44. In the mutant Y222F, the guanidinium of Arg^{220} moves into the space formerly occupied by this water molecule.

When the flavin occupies the outer position, the nitrene is exposed to the solvent and reacts preferentially with water; whereas when the flavin occupies the inner position, the nitrene is more likely to react with the protein. The yield of cross-linked protein was about 80% in the absence of substrate, 66% in the presence of *p*-OHB, and only 17% in the presence of 2,4-DOHB. These results are qualitatively consistent with the flavin positions that are observed in the crystal structures; the flavin occupies the inner position in substrate-free and *p*-OHB–bound forms (*8*).

Anionic inhibitors (*16*) such as Br^- also affect the conformation of the flavin. Structure analysis (Table 1) reveals bromide bound to PHBH at two distinct sites in the vicinity of the flavin (Fig. 4). One site (Br2), near the backbone of residues Ile^{43} and Arg^{44}, is almost fully occupied in all of our experiments and does not appear to influence the flavin position. The other site (Br1), on the *re* side of the flavin (Fig. 4), varies in occupancy according to the distribution of flavin orientations. In the PHBH · *p*-OHB · Br^- structure, in which the flavin adopts the in conformation, a Br^- ion is found at full occupancy in the Br1 site near the *re* side of the flavin. For the PHBH · 2,4-DOHB · Br^- complex, refinement establishes that occupancy of Br^- at the *re* side site (Br1) is about 40%, whereas the occupancy of the in orientation of the flavin is about 20%. Thus, both structures show a linkage between Br^- binding and flavin orientation and suggest that bromide alters the equilibrium between the two conformations of the flavin.

In wild-type PHBH, hydroxylation of the substrate is highly favored, and decay of the flavin C(4a)-hydroperoxide to H_2O_2 and oxidized FAD is not detected (*17*). Formation of product must occur with the flavin in its interior position, with the C(4a)-hydroperoxide positioned to attack the C3 of *p*-OHB, as shown by modeling studies (*6*). At the same time, C(4a) and N(5) are insulated from the solvent, which prevents the competing expulsion of hydrogen peroxide from the FAD, a reaction that entails deprotonation of the N(5)H of the flavin and protonation of the leaving group OOH^- (*4*). With the flavin in the outer position as in the Y222F mutant, N(5)H is exposed to solvent and the flavin hydroperoxide can decay rapidly to hydrogen peroxide and oxidized flavin. Although the mutant Y222F forms flavin hydroperoxide normally, the rate constant for release of H_2O_2 is at least 10 times larger than in wild-type PHBH, and the rate constant for oxygen transfer to the substrate is 15 times smaller. As a result, only 20% of the NADPH consumption is coupled to substrate hydroxylation (Table 2 and Fig. 1). Partial uncoupling of hydroxylation to produce H_2O_2 is also observed in the wild-type enzyme when 2,4-DOHB is used as substrate (*7*). Thus, an increased release of H_2O_2 is associated with the tendency of the flavin to occupy the out position.

Because substrate in solution does not have free access to the active site when the flavin occupies the inner position (Fig. 6A), transient conformational changes, including flavin motion, are expected to accompany substrate binding. Evidence supporting the involvement of isoalloxazine movement in substrate exchange was obtained by observation of the binding of *p*-OHB to wild-type enzyme in which the isoalloxazine ring of 6-azido-FAD had been covalently attached to the protein (*18*). When the flavin is locked in position by cross-linking, the substrate binds with a rate constant of only 0.4 M^{-1} s^{-1}, which is at least 10^7 times slower than the binding of *p*-OHB to the unmodified PHBH (*7*). Thus, even at saturating concentrations (1 mM), binding of substrate with restricted flavin movement is 10^4 times slower than the normal turnover rate. When the flavin is reduced, the on-off rate of substrates is decreased 5000 times (*7*). We attribute this behavior to electrostatic stabilization of the reduced flavin ring in the inner position. The electrostatic potentials in the PHBH dimer and its surroundings, computed by solution of the Poisson-Boltzman equation

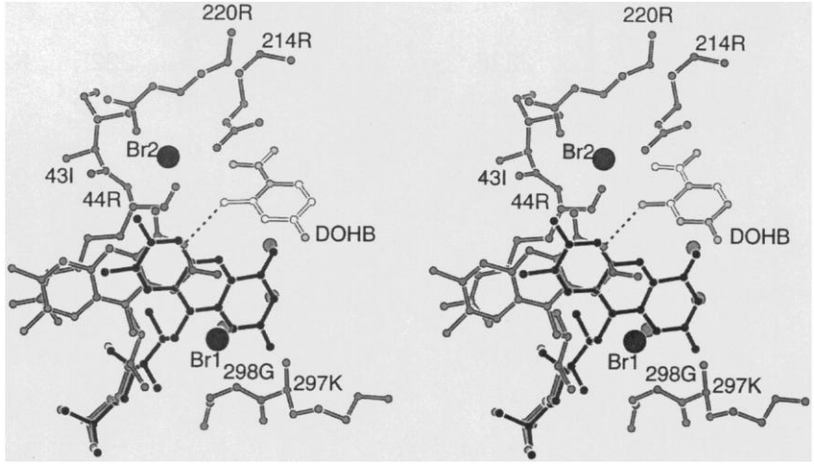

Fig. 4. The wild-type enzyme bound to 2,4-DOHB in the presence of Br^- (*22*). The in orientation of the flavin, which dominates in the complex with *p*-OHB, is drawn with solid bonds. The outer position of the flavin ring (shaded), which is fully occupied in the 2,4-DOHB–PHBH complex, is stabilized by a strong hydrogen bond between the isoalloxazine N(3) and the 2-OH group of the substrate (2.7 Å). The O(4) atom of the outer flavin conformer is 3.0 Å from the hydroxyl of Tyr^{222} (not shown). Three water molecules that are bound in place of the pyrimidine ring when the flavin moves are drawn as shaded circles. Bromide sites, found when Br^- is added to the complex PHBH–2,4-DOHB, are represented by large shaded spheres. When bromide binds at site 2, the Ile^{43}:Arg^{44} peptide rotates by almost 180°. Br^- at site 1 is close to NH 297, NH 298, and a solvent molecule.

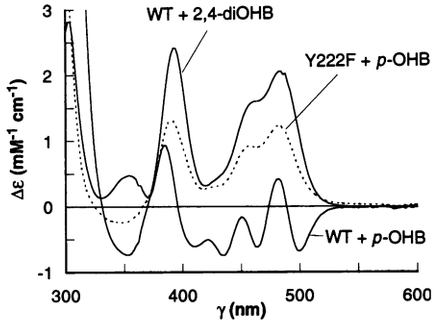

Fig. 5. Difference spectra produced by ligand binding. Each curve was computed by subtraction of the spectrum of the free enzyme from the spectrum of the enzyme after the addition of ligand. Experiments were in 50 mM potassium phosphate and 1 mM EDTA, pH 6.5, at 4°C.

Table 2. Kinetic parameters in wild-type PHBH (WT) and in the mutant Y222F. Activities were measured under standard assay conditions at 25°C. Steady state hydroxylation stoichiometries and single turnover rate constants were measured at pH 6.5 and 3°C as described (*17*).

Enzyme	Relative activity	Hydroxylation of *p*-OHB (%)	Hydroxylation*	H_2O_2 formation*
WT	100	100	46	<1
Y222F	40	20	3.2	9.7

*Rate constants (s^{-1}) were measured for the substrate *p*-OHB.

(*19*), show that the flavin in the inner position is immersed in a core of very positive electrostatic potential, whereas the flavin in the outer position resides in a region of less positive potential. Thus, when the flavin is reduced to its anionic form (*20*) during turnover, electrostatic interactions increase the activation energy required to displace the flavin anion from the well of positive potential, and they inhibit substrate exchange. The equilibrium redox properties of the bound FAD are also consistent with the electrostatic calculations; the redox potential of the bound FAD is about 50 mV more positive than that of the free FAD (*17*), which indicates that the reduced FAD is bound more tightly, by about 2.4 kcal/mol, to the enzyme than is the oxidized form.

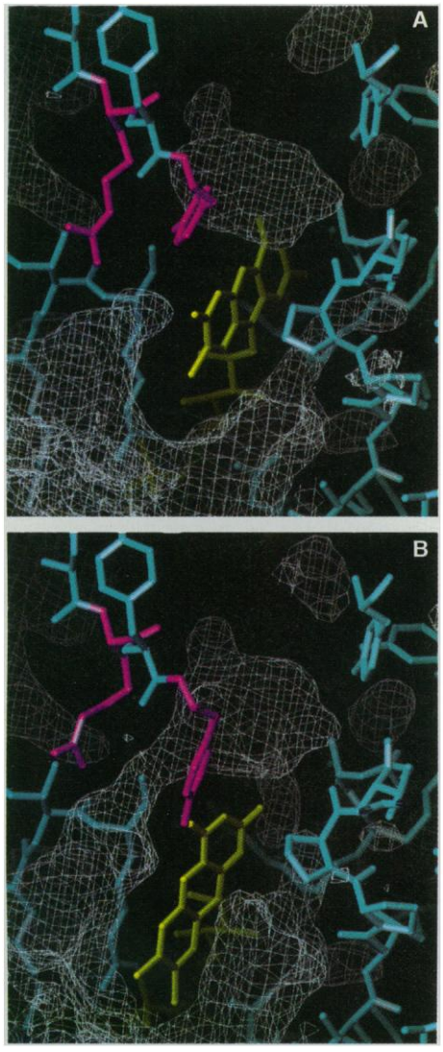

Fig. 6. The active site of PHBH in the "open" and "closed" conformations. Volumes not occupied by protein are contoured in white (*24*). The flavin is shown in yellow. The two residues (Tyr^{222} and Arg^{220}) lining the expected path for the substrate are shown in magenta; other protein residues are in cyan. (**A**) Wild-type enzyme with the flavin occupying the internal position. The isolated pocket where the substrate binds is visible above the flavin. (**B**) Model of the enzyme in which the flavin occupies the external position and Tyr^{222} has been moved away from the substrate (*24*). A channel connecting the surface of the enzyme with the active site pocket is now visible.

All our results thus point to a role for flavin motion in the process of substrate binding or product release in PHBH. In the mutant Y222F, where the hydroxyl of Tyr^{222} is absent, the outer position for the flavin is favored; this suggests that movement of Tyr^{222} (and its hydroxyl group) away from the substrate could facilitate displacement of the flavin in the wild-type enzyme. We modeled a combined rearrangement of FAD and Tyr^{222} that opens a channel from the solvent into the pocket where the substrate binds (Fig. 6B). Although the diameter of the channel in this model is smaller than the substrate, the path may be widened by small transient motions of other groups in the protein. The flexibility of the ribityl side chain is crucial in permitting the flavin to function as a gate that controls the route into and out of the active site. Closing the gate after *p*-OHB binds allows hydroxylation to proceed in a conformation of the active site that protects the intermediates from unwanted reactions with the solvent. Release of the hydroxylated product again requires the opening of the gate, with the flavin swinging out. Similar events may also be important in the binding and release of pyridine nucleotides.

The type of flavin motion described here, on the basis of snapshots of different flavin-binding modes, might well represent a general phenomenon. For instance, the reactions of proton translocation that take place in mitochondrial complex I may include asymmetric protonation and deprotonation of the flavin ring, allowed by a swinging motion of the flavin (*21*). This view emphasizes that the flavin cofactor is widely employed in biological oxidation reactions, not only for its chemical versatility but also for its conformational adaptability.

REFERENCES AND NOTES

1. M. Gerstein, G. Schulz, C. Chothia, *J. Mol. Biol.* **229**, 494 (1993); G. E. Schulz, *Curr. Biol.* **1**, 883 (1991); D. Joseph, G. A. Petsko, M. Karplus, *Science* **249**, 1425 (1990); W. S. Bennett and T. A. Steitz, *Proc. Natl. Acad. Sci. U.S.A.* **75**, 4848 (1978).
2. L. N. Ornston and D. Parke, *Curr. Top. Cell. Regul.* **12**, 209 (1977).
3. D. P. Ballou, in *Flavins and Flavoproteins*, R. C. Bray, P. C. Engel, S. G. Mayhew, Eds. (de Gruyter, Berlin, 1984), pp. 605–618.
4. G. Merényi and J. Lind, *J. Am. Chem. Soc.* **113**, 3146 (1991); T. C. Bruice, *Isr. J. Chem.* **24**, 54 (1984).
5. B. Entsch and D. P. Ballou, *Biochim. Biophys. Acta* **999**, 313 (1989).
6. H. A. Schreuder, W. G. J. Hol, J. Drenth, *J. Biol. Chem.* **263**, 3131 (1988); *Biochemistry* **29**, 3101 (1990).
7. B. Entsch, D. P. Ballou, V. Massey, *J. Biol. Chem.* **251**, 2550 (1976).
8. H. A. Schreuder *et al.*, *Proteins Struct. Funct. Genet.* **14**, 178 (1992); H. A. Schreuder *et al.*, *J. Mol. Biol.* **208**, 679 (1989); H. A. Schreuder, J. M. van der Laan, W. G. J. Hol, J. Drenth, *ibid.* **199**, 637 (1988); R. K. Wierenga, R. J. de Jong, K. H. Kalk, W. G. J. Hol, J. Drenth, *ibid.* **131**, 55 (1979); M. S. Lah, B. A. Palfey, H. A. Schreuder, M. L. Ludwig, *Biochemistry* **33**, 1555 (1994).
9. M. S. Lah, D. Gatti, H. A. Schreuder, B. A. Palfey, M. L. Ludwig, in *Flavins and Flavoproteins 1993*, K. Yagi, Ed. (de Gruyter, Berlin, in press).
10. A. Brünger, *X-PLOR, Version 3.1* (Yale Univ. Press, New Haven, CT, 1992); A. Brünger, A. Krukowski, J. W. Erickson, *Acta Crystallogr.* **A46**, 585 (1990).
11. K. D. Cowtan and P. Main, *Acta Crystallogr.* **D119**, 148 (1993); K. Y. J. Zhang, *ibid.*, p. 213.
12. R. J. Read, *ibid.* **A42**, 140 (1986); *ibid.* **A46**, 900 (1990).
13. C. Cambillau and E. Horjales, *J. Mol. Graph.* **5**, 174 (1987).
14. The FAD of the wild-type enzyme was replaced with 6-azido FAD by application of the enzyme to a column of Red A (Amicon), which had been equilibrated with 10 mM tris maleate and 0.3 mM EDTA (pH 7.0). Under these low ionic strength conditions, the red dye of the column binds the enzyme by displacing FAD. Free flavin was removed by washing the column with the same buffer. The column was further washed with 50 mM potassium phosphate, 0.5 mM EDTA, and 0.5 mM *p*-OHB (pH 7.0), and the enzyme was eluted with the same buffer supplemented with 100 μM 6-azido-FAD. Fractions containing enzyme were concentrated and exchanged into 0.1 M potassium phosphate, pH 7.5, by gel filtration. Photolabeled enzyme was prepared by irradiation of the enzyme in the presence of ligands with a 650-W incandescent lamp at 25°C until the reaction was complete, as monitored spectrally. Flavin that was covalently bound to the enzyme was determined by denaturation of the enzyme with trichloroacetic acid. The precipitated protein was collected by centrifugation and dissolved in 8 M guanidinium hydrochloride. The supernatant was neutralized with NaOH. The amount of flavin in both fractions was estimated spectrally.
15. S. Ghisla, V. Massey, K. Yagi, *Biochemistry* **25**, 3282 (1986).
16. H. Shoun, K. Arima, T. Beppu, *J. Biochem.* **93**, 169 (1983); P. J. Steenis, M. M. Cordes, J. G. H. Hilkens, F. Müller, *FEBS Lett.* **36**, 177 (1973).
17. B. Entsch, B. A. Palfey, M. S. Lumberg, D. P. Ballou, V. Massey, in *Flavins and Flavoproteins 1993*, K. Yagi, Ed. (de Gruyter, Berlin, in press); B. Entsch, B. A. Palfey, D. P. Ballou, V. Massey, *J. Biol. Chem.* **266**, 17341 (1991).
18. Photolabeled enzyme prepared as described (*14*) was separated from the unlabeled enzyme with the use of a Red A column. Covalently modified enzyme did not bind to the column and was eluted in the first wash. The binding of *p*-OHB to covalently labeled enzyme was monitored, in the concentration range 1 to 25 mM, by the absorbance increase at 467 nm in a stopped-flow spectrophotometer. The enzyme was in 0.1 M potassium phosphate, pH 7.5, at 4°C.
19. K. Sharp and B. Honig, *Annu. Rev. Biophys. Biophys. Chem.* **19**, 301 (1990).
20. J. Vervoort, W. J. H. van Berkel, F. Müller, C. T. W. Moonen, *Eur. J. Biochem.* **200**, 731 (1991).
21. P. Mitchell, *Chemiosmotic Coupling in Oxidative and Photosynthetic Phosphorylation* (Glynn Research, Bodmin, UK, 1966); A. D. Vinogradov, *Biophys. J.* **66**, A12 (1994).
22. Abbreviations for the amino acid residues are as follows: F, Phe; G, Gly; I, Ile; K, Lys; L, Leu; N, Asn; R, Arg; S, Ser; V, Val; and Y, Tyr.
23. "Unbiased" electron density showing the flavin ring

occupying two positions in the active site was derived by simulated annealing (with the slow-cool protocol) at 1000 K with the use of X-PLOR (*10*) with the flavin region omitted. Phases were further modified by a full-matrix Sayre refinement with SQUASH (*11*), followed by phase combination with the initial phases derived from simulated annealing. Amplitudes were weighted with SigmaA (*12*).

24. A mask representing the volumes inside the unit cell not occupied by protein was determined with a probe of radius 0.8 Å (*10*). Maps calculated with coefficients derived from the Fourier transform of the mask were contoured at 1 σ. The model of the active site in the "open" conformation was derived from the structure of the enzyme in complex with 2,4-DOHB. The side chain of Tyr^{222} was initially reoriented by manual modeling (*13*), followed by refinement of the atomic coordinates in the CHARMM22 force field in X-PLOR (*10*). Atoms within 5 Å of Tyr^{222} were restrained to their initial positions by application of a harmonic potential. Atoms outside this region were kept fixed during the minimization.

25. Supported by grants from NIH (GM 16429 to M.L.L., GM 20877 to D.P.B., GM 11106 to V.M., and Michigan Molecular Biophysics Training Program GM 08270 to B.A.P.), the University of Michigan (Rackham Graduate School Predoctoral Fellowship to B.A.P. and Rackham Graduate School Program to Support International Partnerships to D.P.B.), and the Australian Research Council (to B.E.). Coordinates have been submitted to the Protein Data Bank.

27 April 1994; accepted 2 August 1994

RNA Editing: Transfer of Genetic Information from gRNA to Precursor mRNA in Vitro

Scott D. Seiwert and Kenneth Stuart*

RNA editing in the mitochondrion of *Trypanosoma brucei* extensively alters the adenosine triphosphate synthase (ATPase) subunit 6 precursor messenger RNA (pre-mRNA) by addition of 447 uridines and removal of 28 uridines. In vivo, the guide RNA gA6[14] is thought to specify the deletion of two uridines from the editing site closest to the 3′ end. In this study, an in vitro system was developed that accurately removed uridines from this editing site in synthetic ATPase 6 pre-mRNA when gA6[14] and ATP were added. Mutations in both the guide RNA and the pre-mRNA editing site suggest that base-pairing interactions control the number of uridines deleted in vitro. Thus, guide RNAs are required for RNA editing and for the transfer of genetic information to pre-mRNAs.

Mitochondrial pre-mRNAs in kinetoplastid protozoa have precise numbers of uridine residues inserted and deleted by RNA editing (k-RNA editing) (*1*). This possibly ancient (*2*) process produces mature mRNA sequences, often creating most of the coding information (*3*, *4*). Small (~60-nucleotide) guide RNAs (gRNAs) have been proposed to specify the sequences of edited transcripts by a combination of Watson-Crick and G:U base pairing (*5*). Most models for k-RNA editing postulate that the 5′ portion of a gRNA initially forms a short (anchor) duplex with the pre-mRNA that it edits and that subsequent editing of the pre-mRNA extends the complementarity of this duplex (*5–7*). Free uridine 5′-triphosphate (UTP) (*5*) or uridine residues at the 3′ end of gRNAs (*6*, *7*) may be the reservoir for the inserted and deleted uridines. As evidence exists in support of both of these possibilities (*7–13*), we developed an in vitro system to analyze the mechanism of k-RNA editing.

Editing of the 3′ end of *Trypanosoma brucei* ATPase 6 pre-mRNA appears to be directed by the gRNA gA6[14] (Fig. 1A) (*14*). The gRNA-mRNA chimeric molecules predicted by some models of RNA editing (*6*, *7*) are produced when these two RNAs are incubated with mitochondrial lysate (*9*). Characterization of these molecules showed that the pre-mRNA portion of several lacked uridine residues at the editing site closest to the 3′ end (ES1), a site from which uridines are deleted in vivo (*4*). Here, we investigated whether removal of these uridines required, and was specified by, the gRNA included in the in vitro incubation, using a procedure analogous to the assay of in vitro RNA editing employed in other systems (*15*). Our assay used dideoxythymidine (ddT) to halt reverse transcription at the adenosine immediately upstream of ES1 in a synthetic ATPase 6 transcript that was modified to distinguish it from endogenous mRNA (A6/TAG; see Fig. 1B) (*16*). A shorter product will be created if the A6/TAG transcript is processed correctly in vitro by gA6[14]. Subsequent treatment with a processive terminal transferase was used to add numerous deoxynucleotides to unextended primer and to products resulting from premature termination and "run-off" reverse transcription (which all terminate in 3′ hydroxyls). Molecules lengthened in such a way are prevented from entering high-percentage polyacrylamide gels, thereby allowing clear identification of extension products terminating in ddT.

Analysis of A6/TAG substrate after coincubation in mitochondrial lysate with an equimolar (Fig. 2, lane 8) or 10-fold molar excess (Fig. 2, lane 9) of synthetic gA6[14] showed two ddT-terminated primer extension products ("product" and "−2" in Fig. 2). Neither resulted from reverse transcription of endogenous RNAs, because neither was seen if A6/TAG was omitted (lane 5). Both products were present after terminal transferase treatment, which nearly completely shifted the unextended primer (compare lanes 1 to 3 with lanes 4 to 10 in Fig. 2, and compare lanes 1 to 3 with lanes 4 to 7 in Fig. 3B). Thus, both bands seen in Fig. 2, lanes 8 and 9, represent primer extension products that terminate in ddT. The upper band represents reverse tran-

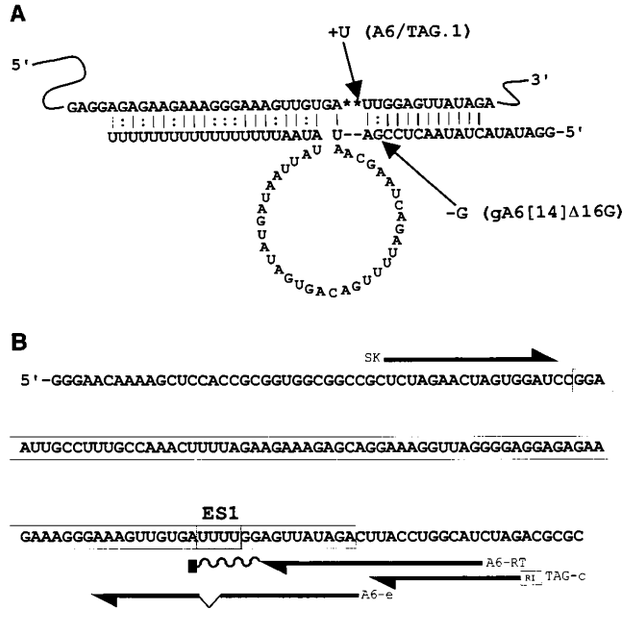

Fig. 1. (**A**) Possible A6/TAG–gA6[14] base pairing. Pre-mRNA is above and gA6[14] below. ES1 is shaded; uridines deleted in vivo are indicated by asterisks. A6/TAG and gA6[14] mutations are indicated by arrows. (**B**) A6/TAG transcript and oligonucleotides. ATPase 6 and heterologous sequence are boxed and unboxed, respectively. ES1 is shaded. Oligonucleotides are indicated as bars, with arrowheads representing 3′ ends. The ddT-terminated primer extension of A6-RT is indicated by a curved line and vertical bar. Oligonucleotide A6-e is complementary to molecules that have two uridines in ES1.

S. D. Seiwert, Department of Molecular Biophysics and Biochemistry, Yale University, New Haven, CT 06536–0182, USA, and Seattle Biomedical Research Institute, Seattle, WA 98109–1651, USA.
K. Stuart, Seattle Biomedical Research Institute, Suite 200, 4 Nickerson Street, Seattle, WA 98109–1651, USA, and Department of Pathobiology, University of Washington, Seattle, WA 98195, USA.
*To whom correspondence should be addressed.